

Arching in tapped deposits of hard disks

Luis A. Pugnaloni,* Marcos G. Valluzzi, and Lucas G. Valluzzi

Instituto de Física de Líquidos y Sistemas Biológicos, UNLP-CONICET, cc. 565, 1900 La Plata, Argentina

(Received 7 January 2006; published 4 May 2006)

We simulate the tapping of a bed of hard disks in a rectangular box by using a pseudodynamic algorithm. In these simulations, arches are unambiguously defined and we can analyze their properties as a function of the tapping amplitude. We find that an order-disorder transition occurs within a narrow range of tapping amplitudes as has been seen by others. Arches are always present in the system although they exhibit regular shapes in the ordered regime. Interestingly, an increase in the number of arches does not always correspond to a reduction in the packing fraction. This is in contrast with what is found in three-dimensional systems.

DOI: [10.1103/PhysRevE.73.051302](https://doi.org/10.1103/PhysRevE.73.051302)

PACS number(s): 81.05.Rm, 81.20.Ev, 83.80.Fg

I. INTRODUCTION

The study of structural properties of assemblies of macroscopic particles packed in a container has become an important area of granular matter. Properties such as packing fraction (ϕ), coordination number (z), and arch distributions depend on the way the packings are created. The so-called “Chicago experiment” [1] has shown that a tapped granular bed can achieve a stationary state where the system characterizing parameters (in this case ϕ) depend only on the tapping amplitude. This simplifies our investigations when we are interested only in the steady state of the system.

Arching is one of the collective phenomena that many associate to the appearance of voids in a granular sample that leads to the lowering of ϕ . Moreover, arching is directly related to the reduction of particle-particle contacts in the assembly, which determines the value of z [2,3]. Arch formation is crucial in the jamming of granular flows [4–7], and it has also been proposed as a mechanism for size segregation [8,9].

Two-dimensional (2D) granular systems merit attention due to the multiple applications in industry and urban life (pills, bottles, etc., on a conveyor belt [10], traffic jams [11], and crowd control [12]) and also due to the possibility of testing theoretical models that are particularly simple to treat in 2D.

Simulation studies of the shaking of 2D granular beds have been carried out by others in the past (see, for example, Ref. [13]). However, these pseudodynamic simulations do not consider simultaneous deposition of the grains. This prevents arching during deposition, which is a main ingredient in granular systems. On the other hand, simulations through realistic granular dynamics have the drawback that there is not a clear criterion to decide when the system is fully deposited, since kinetic energy does not vanishes completely in these simulations. Besides, identifying which particles support a given particle in these type of simulations may prove rather complex.

In this work we study the formation of arches in a 2D assembly of hard disks by using a pseudodynamic simulation

of the tapping and simultaneous deposition of inelastic rough particles. We follow the changes in ϕ , z , and arch properties as a function of the tapping amplitude. Also, an annealed tapping similar to the Chicago experiment is carried out on the system.

II. ARCHING AND COORDINATION NUMBER

Arches are multiparticle structures formed during simultaneous (nonsequential) deposition of an assembly of granular particles. Particles in an arch support each other so that the whole set remains stable against gravity (or the driving force that promotes deposition) [3].

In a two-dimensional bed of convex particles constructed by sequential deposition, the mean coordination number $\langle z \rangle$ is 4: each newly deposited particle adds two contacts—which stabilize the particle—to the system. If particles are deposited nonsequentially, mutual contacts are created where two particles share a stabilizing contact. This diminishes by 1—with respect to a sequential deposition—the total number of contacts in the system and so the value of $\langle z \rangle$ drops. Arches in 2D are string like: any arch has two end particles that share a single mutual contact and a variable number of center particles that share two mutual contacts each. If $n(s)$ is the number of arches consisting of s particles in a system of N particles, there are

$$p_1 = 2 \sum_{s=2}^N n(s) \quad (1)$$

end particles and

$$p_2 = \sum_{s=3}^N (s-2)n(s) \quad (2)$$

center particles in the assembly. Here, $n(s=1)$ corresponds to the number of particles that do not belong to any arch. Therefore, the mean coordination number can be obtained as

$$\langle z \rangle_{\text{support}} = 4 - \frac{p_1}{N} - 2 \frac{p_2}{N}. \quad (3)$$

We use the subscript “support” because this coordination number does not take into account the existence of nonsup-

*Email address: luis@iflysis.unlp.edu.ar

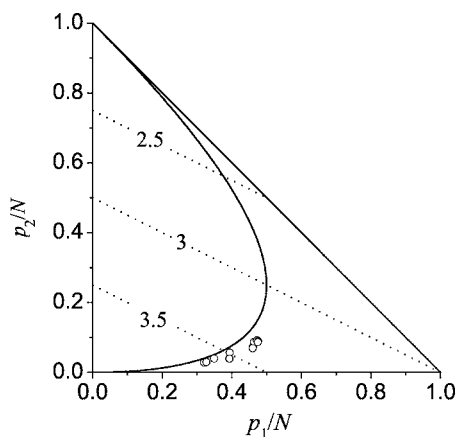


FIG. 1. Mutual stability phase diagram for 2D packings. Here, p_1/N and p_2/N are the fractions of particles that present one and two mutually stable supporting contacts, respectively. The state point of any packing must lie in the triangle defined by $(0,0)$, $(0,1)$, and $(1,0)$. The dotted lines correspond to states of equal $\langle z \rangle_{\text{support}}$ (the numbers indicate the corresponding values). The solid curve represents all the states that can be obtained through the exponential model (see text). Open circles correspond to a representative sample of the packings generated in our simulations.

porting contacts. In nonsequentially deposited beds there will be some contacts that do not serve to the stability of any of the two touching particles. In our simulations, these nonsupporting contacts represent least than 0.3% of the contacts. Using Eqs. (1)–(3) and after some algebra we obtain

$$\langle z \rangle_{\text{support}} = 2 \left[1 + \frac{1}{N} \sum_{s=1}^N n(s) \right]. \quad (4)$$

The analysis above can be done also in 3D but it requires more complex expressions due to the fact that arches can present branches [2,3,14].

Bearing in mind that $\sum_{s=1}^N sn(s) = N$, we can model $n(s)$ as a simple exponential decay in the limit $N \rightarrow \infty$ —i.e.,

$$n(s)/N = 2(\cosh[\alpha] - 1)\exp[-\alpha s], \quad (5)$$

with α a positive number. In this model we obtain

$$\langle z \rangle_{\text{support}} = 4 - 2 \exp[-\alpha]. \quad (6)$$

The exponential model seems to work well for stringlike bridges in 3D (see Ref. [14]). We will see below that, in 2D, this is only a rough model for $n(s)$ according to our simulation results. However, from Eq. (6) we can already observe that $\langle z \rangle_{\text{support}}$ can only vary between 2 and 4 in 2D. Notice that this result does not depend on the shape of the particles as long as they are convex and support each other through point contacts. The case $\langle z \rangle_{\text{support}} = 2$ corresponds to a very particular configuration where all particles belong to a single large arch. This, of course, is impossible to achieve with walls present.

In a graph of p_2/N as a function of p_1/N (see Fig. 1) any packing must belong to the triangle $[(0,0), (0,1), (1,0)]$ and the lines parallel to the segment $[(0,0.5), (1,0)]$ correspond to states of equal $\langle z \rangle_{\text{support}}$. The curve shown in Fig. 1 corre-

sponds to the loci of the states given by the exponential model of $n(s)$ with α ranging from 0 to ∞ . In practice, $\langle z \rangle_{\text{support}}$ only ranges from 3 to 4 (see the simulation data point in Fig. 1). The lower limit ($\langle z \rangle_{\text{support}} = 3$) has been suggested to correspond to the marginally rigid state in 2D [15].

III. SIMULATION DETAILS

Our simulations are based on an algorithm for inelastic hard disks designed by Manna and Khakhar [17,18]. This is a pseudodynamics that consists in small falls and rolls of the grains until they come to rest by contacting other particles or the system boundaries. We use a container formed by a flat base and two flat vertical walls. No periodic boundary conditions are applied. Once all the grains come to rest, the system is expanded and randomly shaken to simulate a vertical tap. Then, a new deposition cycle begins. After several taps, the system achieves a steady state where all characterizing parameters fluctuate around an equilibrium value.

The deposition algorithm consists in picking up a disk in the system and performing a free fall of length δ if the disk has no supporting contacts, or a roll of arclength δ over its supporting disk if the disk has one single supporting contact [17,18]. Disks with two supporting contacts are considered stable and left in their positions. If in the course of a fall of length δ a disk collides with another disk (or the base), the falling disk is put just in contact and this contact is defined as its *first supporting contact*. Analogously, if in the course of a roll of length δ a disk collides with another disk (or a wall), the rolling disk is put just in contact. If the *first supporting contact* and the second contact are such that the disk is in a stable position, the second contact is defined as the *second supporting contact*; otherwise, the lowest of the two contacting particle is taken as the *first supporting contact* of the rolling disk and the *second supporting contact* is left undefined. If, during a roll, a particle reaches a lower position than the supporting particle over which it is rolling, its *first supporting contact* is left undefined. A moving disk can change the stability state of other disks supported by it; therefore, this information is updated after each move. The deposition is over once each particle in the system has both supporting contacts defined or is in contact with the base (particles at the base are supported by a single contact). Then, the coordinates of the centers of the disks and the corresponding labels of the two supporting particles, wall, or base are saved for analysis.

The tapping of the system is simulated by multiplying the vertical coordinate of each particle by A (with $A > 1$). Then, the particles are subjected to several (about 20) Monte Carlo loops where positions are changed by displacing particles a random length Δr uniformly distributed in the range $0 < \Delta r < A - 1$. New configurations that correspond to overlaps are rejected. This disordering phase is crucial to avoid particles falling back again into the same positions. Moreover, the upper limit for Δr (i.e., $A - 1$) is deliberately chosen so that a larger tap promotes larger random changes in the particle positions.

The simulations are carried out in a rectangular box of width 20 containing 2000 equal-sized disks of radius $r = 0.1$

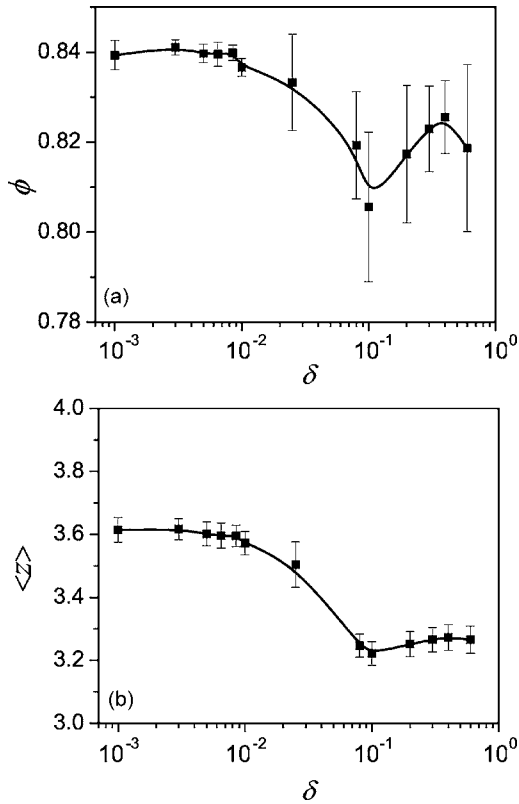


FIG. 2. Packing fraction (a) and $\langle z \rangle_{\text{support}}$ (b) as a function of the parameter δ of the simulation algorithm for $A=1.1$. Solid lines are only to guide the eye.

$+1/\sqrt{2} \approx 0.807$. The disk size is chosen in such way that the neighbor-linked-cell system used to speed up the simulation contains a single particle per cell. Initially, disks are placed at random in the simulation box (with no overlaps) and deposited using the pseudodynamic algorithm. Then, 10^3 tapping cycles are performed for equilibration followed by 10^3 taps for production; saving only 1 every 10 fully deposited configurations. Tapping amplitudes range from 1.02 up to 2.0. Enlarging the width of the simulation box up to 30 has shown no effect on the results that we present here. The same is true if one reduces the number of particles down to 500.

An important point in this simulations is the effect that the parameter δ has in the results since particles do not move simultaneously but one at a time. One might expect that in the limit $\delta \rightarrow 0$ we should recover a fairly “realistic” dynamics for a fully inelastic rough disk dragged downwards at constant velocity. This should represent particles deposited in a viscous medium or carried by a conveyor belt. In Fig. 2, we show ϕ and $\langle z \rangle_{\text{support}}$ for $A=1.1$ as a function of δ . As we can see, the results are independent of δ for small values of the parameter. Since computation efficiency decreases with decreasing δ —due to the number of free falls required for the particles to come together at the bottom of the container—we choose the largest value that yield results indistinguishable from the small- δ limit within statistical errors (i.e., $\delta=0.01$). This value might be inappropriate for simulations with small values of A . We have checked that results are consistent in such simulations by reducing δ up to an order of magnitude.

The deposited configurations are analyzed in search of arches. We first identify all mutually stable particles—which

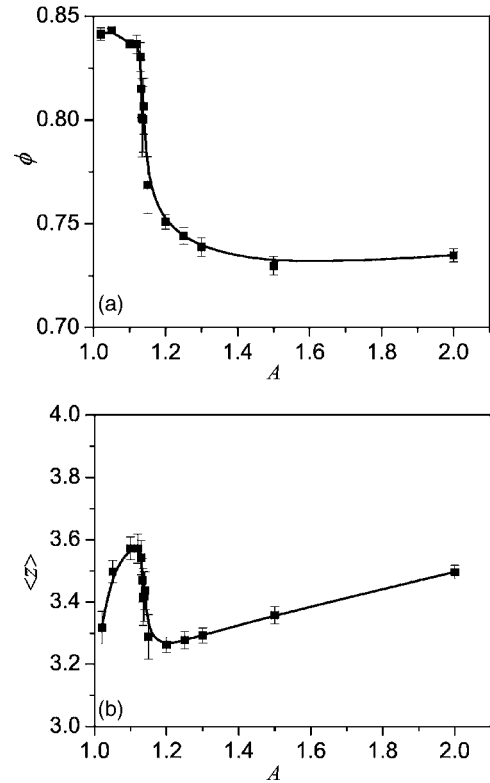


FIG. 3. Packing fraction (a) and $\langle z \rangle_{\text{support}}$ (b) as a function of the tapping amplitude A .

we define as directly connected—and then we find the arches as chains of connected particles. Two disks A and B are mutually stable if A is the left supporting particle of B and B is the right supporting particle of A or vice versa. We measure the total number of arches, arch size distribution $n(s)$, and the horizontal span distribution of the arches $n_s(x)$. The latter is the probability density of finding an arch consisting of s disks with horizontal span between x and $x+dx$. The horizontal span (or lateral extension) is defined as the projection onto the horizontal axis of the segment that joins the centers of the right-end disk and the left-end disk in the arch.

IV. RESULTS

In Fig. 3 we show the area fraction (or packing fraction) ϕ occupied by the disks as a function of the tapping amplitude. We also plot, in Fig. 3, $\langle z \rangle_{\text{support}}$ as a function of A . We can identify four parts in Fig. 3(a). For small values of A (up to about 1.1), the area fraction falls very slowly from just above 0.84 to around 0.83. In the range $1.1 < A < 1.15$, simulations present large fluctuations but a sharp drop is observed, with ϕ ranging between 0.76 and 0.83. Then, in the range $1.15 < A < 1.5$ there is a mild decrease in ϕ . Finally, for $A > 1.5$, we can observe in Fig. 3(a) a very slow rise in ϕ .

The sharp change in ϕ around $A=1.13$ has been described previously as an order-disorder transition due to the crystallization of the disks into a triangular lattice. This transition has been located around $\phi=0.8$ by experiments [19], which agrees with our simulations. The maximum value of ϕ in the

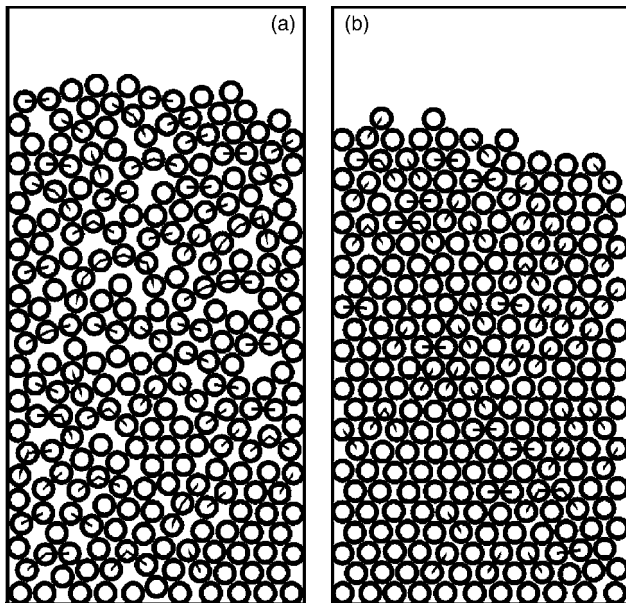


FIG. 4. Examples of the packings. (a) 250 particles tapped with $A=1.3$ which corresponds to the disordered regime. (b) 250 particles tapped with $A=1.1$ which corresponds to the ordered regime. Arches are indicated by segments joining mutually stable particles.

crystalline regime depends strongly on the ratio between the box width and the diameter of the disks. For integer ratios, the crystal can achieve the smallest lattice constant, hence the highest packing fraction. We do not commensurate our box to the particle size since this situation is difficult to achieve in experiments anyway.

The slow increase in ϕ for very large tapping amplitudes is consistent with experiments carried out using noncircular particles “deposited” by a conveyor belt in a \sqcup -shaped container [15]. In this regime, we expect ϕ to slowly approach the value of sequentially deposited disks (i.e., $\phi \approx 0.82$ [21]), since a very strong tap should separate out the disks to such degree that they will fall back without many multi-particle collisions.

In Fig. 4 we show two examples of packings with 250 particles corresponding to the disordered [Fig. 4(a)] and the ordered [Fig. 4(b)] regimes. Arches are indicated with segments that join mutually stable particles. It is important to notice here that in our simulations particles that reach the base “stick” to their positions and are not pushed aside by further colliding disks during deposition. This prevents the formation of completely regular crystals since the first layer is already a randomly deposited layer. In a proper granular dynamic simulation one obtains more ordered structures [20]. Our ordered regime is better described as a layering of the system rather than a crystallization. This is indeed a limitation of the model since most 2D granular beds tend to present crystal-like order in real life.

It is interesting to see whether in the transition region ($1.1 < A < 1.15$) the system presents a phase separation type behavior. We have plotted the profile of ϕ in the vertical (y) direction for some tapping amplitudes in Fig. 5. In the disordered regime, with exception of several bottom layers, the system shows a constant $\phi(y)$ (with values below 0.8). In the

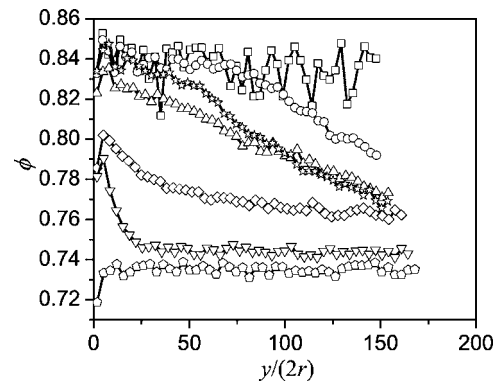


FIG. 5. Vertical profile of the packing fraction for various values of A : squares (1.1), circles (1.13), up triangles (1.135), stars (1.14), diamonds (1.15), down triangles (1.25), and pentagons (2.0).

ordered regime, the system has also a constant $\phi(y)$ (with values around 0.84). Within the transition region, however, the profile shows a monotonic decrease from orderedlike area fractions down to disorderedlike densities. We have found no sign of a stepwise profile which would indicate a coexistence between an ordered phase and a disordered phase.

The most striking results from our simulations is the behavior of $\langle z \rangle_{\text{support}}$ as a function of A [see Fig. 3(b)]. Here, we can identify only three distinct parts. For small A (within the ordered region), $\langle z \rangle_{\text{support}}$ grows with A . This implies that larger tapping amplitudes “destroy” mutual contacts in the ordered phase. Interestingly, at the order-disorder transition, $\langle z \rangle_{\text{support}}$ presents a sharp drop. This may be attributed to the appearance of many arches in the system that lead to the loss of order. Finally, within the disordered region, the system increases its coordination linearly with A . This last observation is consistent with experiments in 2D of particles “deposited” by a conveyor belt [15]. Clearly, arches are always present in the system since $\langle z \rangle_{\text{support}} < 4$ in all cases. The striking feature is the nonmonotonic behavior of $\langle z \rangle_{\text{support}}$. Starting from small tapping amplitudes one can remove mutual contacts (and hence arches) by increasing A . However,

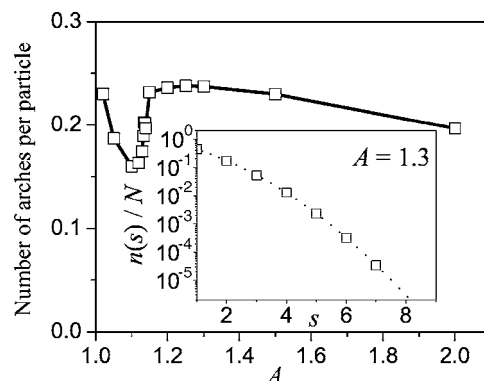


FIG. 6. Number of arches per unit particle as a function of the tapping amplitude. The solid line is only a guide to the eye. The inset shows a semilog plot of the arch size distribution $n(s)$. Symbols correspond to our simulations for $A=1.3$ and the dotted line to a fit with a second order polynomial.

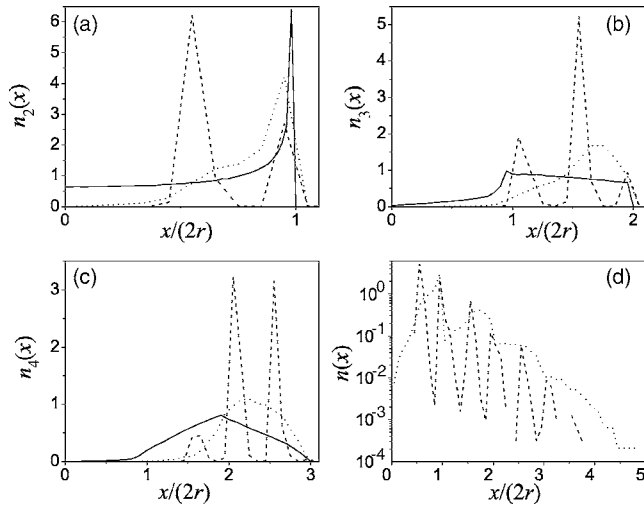


FIG. 7. Distribution of the horizontal span $n_s(x)$ of the arches: (a) arches with two disks, (b) arches with three disks, and (c) arches with four disks. Part (d) corresponds to the horizontal span distribution over all arches. The dotted line corresponds to $A=1.2$. The dashed line corresponds to $A=1.1$. Solid line corresponds to the restricted random walk model (see Ref. [4]).

at the order-disorder transition a small increase in A leads to the creation of many new mutual contacts. Once in the new disordered regime, one can again remove mutual contacts by a further increase in A . Unfortunately, we are unable to support these findings with experimental evidence (apart from the behavior in the disordered regime that agrees with Blumenfeld *et al.*[15]) since coordination numbers are rarely obtained in experiments. It is worth pointing out that simulations of 3D systems show a monotonic *decrease* (not increase) in $\langle z \rangle$ as A is increased (see, for example, Ref. [16]).

From Eq. (4) we know that an increase in the number of arches in the system necessarily leads to a decrease of $\langle z \rangle_{\text{support}}$. This can be seen by comparing Fig. 3(b) with Fig. 6 where we plot the total number of arches per particle versus A . Of course, we see again a sudden change at the order-disorder transition. Arches are more rare in the ordered phase just before the transition to the disordered phase. As we mentioned, in both regimes (ordered and disordered), arches are “destroyed” by increasing the tapping amplitude.

It is commonly said that arches are responsible for voids in a granular pack which, in turn, diminish ϕ . However, from our results we can conclude that, in 2D, this is only true within the order-disorder transition region ($1.1 < A < 1.15$) and for very large tapping amplitudes ($A > 1.5$). In both cases a decrease in the number of arches corresponds to an increase in the packing fraction and vice versa. In contrast, for the rest of the packings (i.e., for $A < 1.1$ and $1.15 < A < 1.5$), a decrease in the number of arches coincides with a decrease in the packing fraction. This result may seem rather counter-intuitive; however, is not just the number of arches but their geometrical properties that determine the total volume of the voids left beneath them. Let us remind ourselves that random packings of disks containing no arches at all (i.e., $\langle z \rangle_{\text{support}} = 4$) have $\phi \approx 0.82$ [21], which is lower than our arch-containing ordered packings and higher than our arch-containing disordered packings.

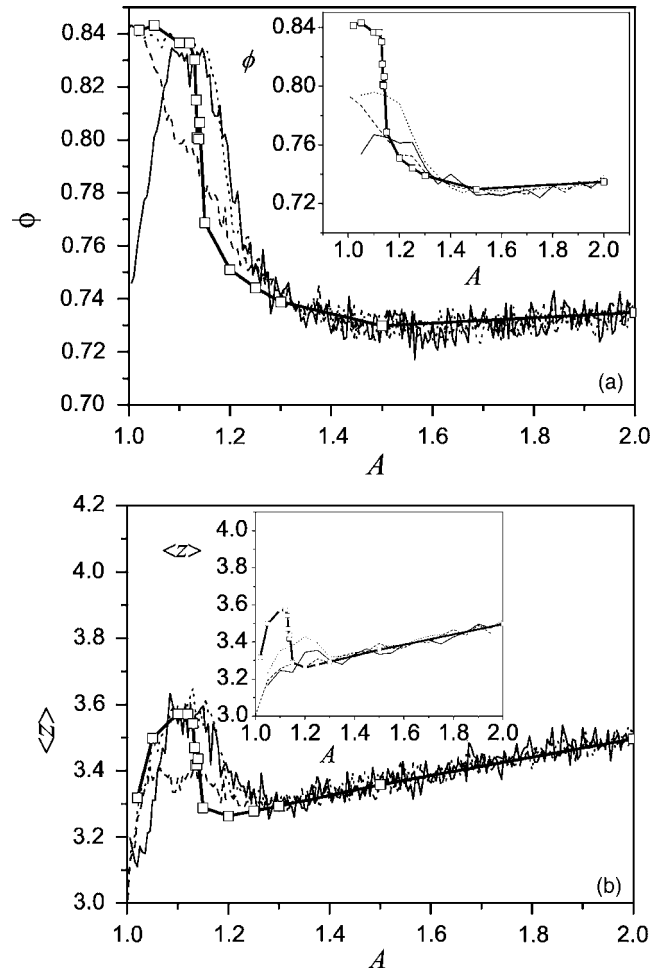


FIG. 8. Packing fraction (a) and $\langle z \rangle_{\text{support}}$ (b) as a function of the tapping amplitude A along an annealed tapping. Tapping amplitude is increased and decreased several cycles. Each increasing (decreasing) cycle takes 2000 taps. As a reference, we show the steady state obtained through constant tapping amplitude with symbols and solid thick line (see Fig. 3). The solid thin line corresponds to the initial increase of A . The dashed line corresponds to the decreasing phase and the dotted line to the increasing phase. All increasing cycles (apart from the initial increase) are averaged to produce a single curve. The same is done with the decreasing cycles. The insets show results where each increasing (decreasing) cycle is performed in only 200 taps.

In the inset of Fig. 6 we show the arch size distribution $n(s)$. This distribution is rather insensitive to A ; hence, we plot $n(s)$ for a single tapping amplitude. Since $\langle z \rangle_{\text{support}}$ depends on the sum of $n(s)$ through Eq. (4), small variations of $n(s)$ that are not appreciable in a semilog plot promote significant changes in $\langle z \rangle_{\text{support}}$. The arch size distribution can be fitted very well to a parabola in a semilogarithmic plot. However, this fitting can only be extended up to $s=7$ or 8 , since we find no arches with more than eight disks in our simulations. Presumably, simulations with a larger number of particles and a wider container will occasionally present larger arches. From Fig. 6, we can see that the simple exponential model we presented above is not suitable to describe arch distributions in 2D packings.

We have also analyzed the horizontal span of the arches. In Fig. 7 we represent $n_s(x)$ for $s=2$ (a), 3 (b), and 4 (c) and the horizontal span $n(x)$ averaged over all arches [Fig. 7(d)]. We include results from two simulations just before and after the order-disorder transition along with the theoretical model presented by To *et al.* [4] based on a restricted random walk. In the case of $n(x)$ we have no theoretical prediction since a theoretical model for $n(s)$ is needed to weight the contributions of each size of arch.

In the ordered regime, we can appreciate a clear discretization of the arch extensions. This is easily understood since in the ordered state particles—even those forming arches—are organized in layers. Arches consisting of two disks, for example, can be formed by two disks at the same layer [corresponding to the peak near $x=1.0$ in Fig. 7(a)] or by one disk in one layer and another disk in the next layer displaced half “lattice constant” in x (corresponding to the peak near $x=0.5$). This argument can be extended to larger arches. See Fig. 4(b) to appreciate the form of the arches in the ordered regime.

In the disordered regime, arches have no distinct lateral extensions but a continuous distribution. This is in agreement with the simple model by To *et al.* which was actually designed to represent arches at the outlet of a hopper. However, our arches tend to be more extended than those from the restricted random walk model. In particular, for two-disk arches, we have no incidence of zero lateral span (corresponding to one disk on top of the other) in contrast with the model.

Finally, in order to check the ability of the simulation model to reproduce some features typical of granular materials, we have also performed an annealed tapping on the system. We have increased and decreased A progressively (from 1.0 to 2.0) 5 times and have plotted ϕ and $\langle z \rangle_{\text{support}}$ as a function of A , averaging all A -increasing cycles and all A -decreasing cycles separately. The very first A -increasing cycle is kept aside. Each increase from $A=1.0$ to $A=2.0$

takes 2000 taps. The results in Fig. 8 correspond to averages over 5 independent simulations using 500 particles. For reference, we include the steady state curves obtained at constant tapping amplitude from Fig. 3. The inset shows results where the ramp rate is increased so that each cycle takes only 200 taps instead of 2000.

According to Nowak *et al.* [1], after the very first increasing cycle, a granular bed should enter a reversible regime where further cycles of the tapping amplitude follow the same curve in the ϕ - A plot. However, Mehta and Barker [22] found in their 3D simulations a hysteresis loop and suggest that the area of the loop should increase as the ramp rate is increased. We also find hysteresis in our 2D simulations. However, increasing the ramp rate does not clearly enlarge the hysteresis loop. The most clear change due to the increase in ramp rate is the difficulty that the system finds in reaching the ordered regime. This is in agreement with the experiments by Nowak *et al.* where an increase in the ramp rate leads to lower densities in the small- A limit.

V. CONCLUSIONS

We have shown through a pseudodynamic simulation that arches are ubiquitous in a 2D granular packing. Very light tapping of the granular sample promotes layering of the particles. The transition from large-amplitude tapping (disordered packings) to small-amplitude tapping (ordered packings) is very sharp and occurs without a phase separation mechanism. Interestingly, we found that in a wide range of tapping amplitudes an increase in the number of arches coincides with an increase of the density of the packing. With exception of the order-disorder transition region, the mean coordination number is always increased by increasing the tapping amplitude, in contrast to what is found in 3D packings.

ACKNOWLEDGMENT

This work has been supported by CONICET of Argentina.

-
- [1] E. R. Nowak, J. B. Knight, M. Povinelli, H. M. Jaeger, and S. R. Nagel, *Powder Technol.* **94**, 79 (1997).
 - [2] L. A. Pugnaloni, G. C. Barker, and A. Mehta, *Adv. Complex Syst.* **4**, 289 (2001).
 - [3] L. A. Pugnaloni and G. C. Barker, *Physica A* **337**, 428 (2004).
 - [4] K. To, P.-Y. Lai, and H. K. Pak, *Phys. Rev. Lett.* **86**, 71 (2001).
 - [5] K. To, *Phys. Rev. E* **71**, 060301(R) (2005).
 - [6] I. Zuriguel, L. A. Pugnaloni, A. Garcimartín, and D. Maza, *Phys. Rev. E* **68**, 030301(R) (2003).
 - [7] I. Zuriguel, A. Garcimartín, D. Maza, L. A. Pugnaloni, and J. M. Pastor, *Phys. Rev. E* **71**, 051303 (2005).
 - [8] J. Duran, J. Rajchenbach, and E. Clément, *Phys. Rev. Lett.* **70**, 2431 (1993).
 - [9] J. Duran, T. Mazozi, E. Clément, and J. Rajchenbach, *Phys. Rev. E* **50**, 5138 (1994).
 - [10] R. Mattone, M. Divona, and A. Wolf, *Rob. Comput.-Integr. Manufact.* **16**, 73 (2000).
 - [11] D. Helbing and B. A. Huberman, *Nature (London)* **396**, 738 (1998).
 - [12] D. Helbing, I. J. Farkas, and T. Vicsek, *Nature (London)* **407**, 487 (2000).
 - [13] A. M. Vidales, V. M. Kenkre, and A. Hurd, *Granular Matter* **3**, 141 (2001).
 - [14] A. Mehta, G. C. Barker, and J. M. Luck, *J. Stat. Mech.: Theory Exp.* (2004) P10014.
 - [15] R. Blumenfeld, S. F. Edwards, and R. C. Ball, *J. Phys.: Condens. Matter* **17**, S2481 (2005).
 - [16] A. Mehta and G. C. Barker, *Rep. Prog. Phys.* **57**, 383 (1994).
 - [17] S. S. Manna and D. V. Khakhar, *Phys. Rev. E* **58**, R6935 (1998).
 - [18] S. S. Manna, *Phase Transitions* **75**, 529 (2002).
 - [19] I. C. Rankenburg and R. J. Zieve, *Phys. Rev. E* **63**, 061303 (2001).
 - [20] R. Arévalo *et al.* (unpublished).
 - [21] G. C. Barker and M. J. Grimson, *J. Phys.: Condens. Matter* **1**, 2779 (1989).
 - [22] G. C. Barker and A. Mehta, *Phase Transitions* **75**, 519 (2002).